Acta Cryst. (1975). B31, 2444

Comparison of Observed and Predicted Structural Parameters of Mica at High Temperature

BY HIROSHI TAKEDA

Mineralogical Institute, Faculty of Science, University of Tokyo, Hongo, Tokyo 113, *Japan*

AND BRUNO MOROSIN

Sandia Laboratories, Albuquerque, New Mexico 87115, *U.S.A.*

(*Received* 13 *January* 1975; *accepted* 10 *April* 1975)

A geometrical model structure for trioctahedral micas has been applied to predict the structural changes of a synthetic fluorphlogopite, $KMg_3(Si_3Al)O_{10}F_2$, as a function of temperature and these are compared with observed structural parameters determined at 700°C. The model employs the cell dimensions measured as a function of temperature, the bond lengths determined at room temperature and thermal expansion coefficients of the bond lengths determined in previous studies. The predicted tetrahedral rotation angle, α, suggests that the silica oxygen ring about the potassium becomes more nearly hexagonal at higher temperatures. The mode of expansion of the Mg octahedron changes at about 400°C, whereafter the octahedron tends to become elongated along the normal to the layer formed by the octahedra. This change in the mode of expansion corresponds to the observed kink in the linear expansivities of the cell dimensions. The predicted parameters have been confirmed by a structure refinement on data collected at 700°C. The observed α (3°) and octahedral flattening angles for magnesium (58·0°) and for potassium (56·5°) at 700°C agree with the predicted values. The very large expansion coefficient of the K–O bond length accounts for large linear expansivity along **c**.

Introduction

The dimensional misfit between the octahedral and tetrahedral layers in both dioctahedral and trioctahedral micas was treated extensively by Radoslovich & Norrish (1962) on the basis of a detailed analysis of the muscovite structure (Radoslovich, 1960). A method of modeling the trioctahedral mica structure using cell dimensions and chemical composition (Donnay, Donnay & Takeda, 1964) has been successfully applied to elucidate continuous structural changes in many mica solid-solution series; examples which may be cited include lithium fluorphlogopite (Takeda & Donnay, 1966), polylithionite (Takeda & Burnham, 1969), and the biotite series (Takeda & Morimoto, 1970). Furthermore, the method was applied to many synthetic micas by Hazen & Wones (1972) and to phlogopite and annite by Hazen & Burnham (1973). A similar approach has been extended to brittle micas as well as other layered silicates by Takéuchi (1964). Recently an improvement was made to such models by taking into account the shortening of the basal O–O distances of the tetrahedra (Takeda, 1971). Similar approaches were also made to obtain better predictions of α, the rotation of the tetrahedral groups around **c***, by Drits (1969), and McCauley & Newnham (1971); however, these authors included more observed parameters such as z coordinates of the oxygen atoms.

Furthermore, the structure of a high-pigeonite determined at 900°C (Smyth & Burnham, 1972) revealed in pyroxenes differences in the mean thermal expansivities (differential expansion) of various polyhedra. The same phenomena were investigated for pyroxenes and amphiboles in detail by other investigators (Cameron, Sueno, Prewitt & Papike, 1973; Sueno, Cameron, Papike & Prewitt, 1973). The expansions of the octahedra give rise to an extension of the tetrahedra forming the silicate chain attached to them. Such structural rearrangements are exactly those previously postulated by us for the mica structure whenever an expansion of the octahedron results from substitution with a larger cation. Similar structural rearrangements as a function of temperature and the effect of impurity substitutions on such rearrangements has also been noted in beryl by Morosin (1972).

In this paper we have applied the improved geometrical model structure, using the observed lattice constants of a fluorphlogopite as a function of temperature together with room temperature bond lengths and mean thermal expansivities for similar bond lengths, to calculate some model structural parameters of fluorphlogopite at high temperatures. We then compare such predicted structure parameters (α, ψ, φ and interatomic distances as defined below) with values calculated using parameters obtained by the refinement of Mo $K\alpha$ intensity data taken at 700°C. The closely related structural expansion resulting from chemical substitution with larger cations is also discussed.

Geometrical model structure used for prediction

The geometrical model structure used in this paper has evolved through various steps and is based on

several refined structures of the trioctahedral micas. Radoslovich & Norrish (1962) examined in detail a mechanism by which the ideal hexagonal ring of the tetrahedra deforms into a ditrigonal ring so as to compensate for the dimensional 'misfit' between the tetrahedral layer and the octahedral layer, and proposed a method of calculating the rotation of silica tetrahedra. This was followed by the first generalized model structure proposed by Donnay *et al.* (1964) who introduced an angle to express the flattening of the octahedral sheet. Recently, Hazen & Burnham (1973) cited formulae for calculating the values of the observed angles. Donnay *et al.* (1964) formulated a set of basic mathematical relationships for predicting structural parameters by utilizing the geometrical relations inherent to the model. Included in these relationships are the following needed for the present study:

$$b = 4\sqrt{2}d_t \cos\alpha \qquad (1)$$

$$b = 3\sqrt{3}d_o \sin\psi \qquad (2)$$

$$\sin^2\psi = 4/[3(1+r_o^2)],$$

where b is the cell dimension, d_t is the tetrahedral cation to oxygen distance, d_o is the octahedral cation to anion distance, α is the rotation of the tetrahedral groups about **c*** defining the degree of deformation from a hexagonal to a ditrigonal ring for the silica oxygen about the potassium ion (Fig. 1), ψ is an angle describing the degree of flattening of the octahedron along the $\bar{3}$ axis (see Fig. 2 of Donnay *et al.*, 1964), and r_o is the ratio of the lengths of the shared O–O edge to the unshared O–O edge of the octahedron. Equations (1) and (2) define the orientational and distortional relationships required so that the tetrahedra, by rotation of α degrees, and the octahedra, by flattening to ψ degrees, will fit an observed b axis length for given d_t and d_o (see Fig. 3 of Donnay *et al.*, 1964). The physical significance of postulating such a model can be understood by the fact that the potential minimum describing the cation–anion bond is very narrow and deep, whereas that for the anion–anion interaction is very shallow and wide.

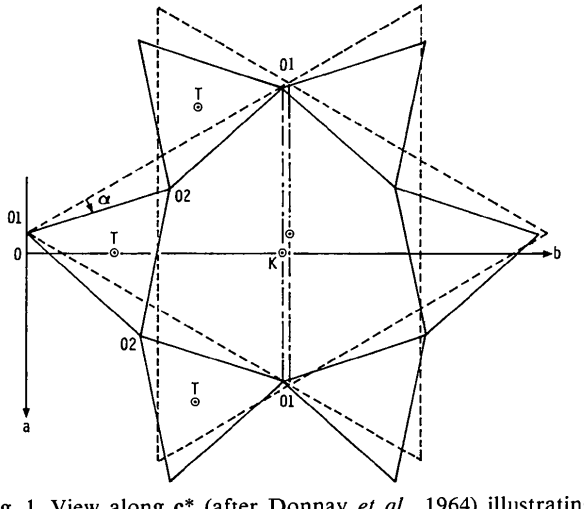

Fig. 1. View along **c*** (after Donnay *et al.*, 1964) illustrating the arrangement of silica tetrahedra about the potassium ion in the mica layer. These tetrahedra rotate slightly with decreasing temperature from the idealized high-temperature form (dotted lines) to that found at room temperature (solid lines). The angle α defines the rotation of these tetrahedra from the ideal hexagonal to a ditrigonal ring which the silica oxygens form about the potassium ion.

Predicting the value of α has been the subject of extensive study during the last decade. There have been various other model structures proposed (Franzini & Schiaffino, 1963; Drits, 1969; Tepikin, Drits & Alexandrova, 1969; McCauley & Newnham, 1971) which require the inclusion of more observed information in order to improve the predicted value of α. Most such approaches necessitate that all of the mica structures be determined in order to obtain the final model. It is our present intent to employ a model with fewer empirical factors.

A major discrepancy found in predicting the value of α, especially for some micas with small α values, results from the smaller size of the basal oxygen triangle of the tetrahedral layer (Tepikin *et al.*, 1969; Takeda & Burnham, 1969). Takeda (1971) derived a correction factor to be applied to the generalized model structure of Donnay *et al.*, (1964) of the form $r_t = e_b/e_l$, where e_b is the basal O–O distance and e_l is the lateral O–O distance (Fig. 2). It is evident from Fig. 2 that the mean tetrahedral edge length e and the height of tetrahedron t can be expressed in terms of e_b and e_l as:

$$e = (e_l + e_b)/2$$

and

$$t^2 = e_l^2 - \tfrac{1}{3}e_b^2 .$$

From these equations, the value of α and t for the deformed tetrahedron can be expressed in terms of d_t as:

$$e_b = Ee = 2\sqrt{\tfrac{2}{3}}Ed_t$$

$$t = 4Hd_t/3$$

$$\cos\alpha = b/(2\sqrt{3}e_b)$$

where E and H are the correction factors to be applied for e and t and determined as:

$$E = 2r_t/(1+r_t)$$

$$H = \sqrt{6-2r_t^2}/(1+r_t) .$$

The values of r_t are not a simple function of the known parameters, but can be generally approximated in terms of the d_t(apical)/d_t(mean) ratio, the value depending mainly on the aluminum content in the tetrahedra (Fig. 3).

With these correction factors, all the equations necessary for predicting the structural parameters of micas can be summarized as:

$$\tan\alpha = 4\sqrt{2}E[(d_t/b)^2 - 1/(4\sqrt{2}E)^2]^{1/2} \quad (3)$$

$$d_o\cos\psi = b[(d_o/b)^2 - \tfrac{1}{27}]^{1/2} \quad (4)$$

$$(\text{K–O})^2_{\text{in}} = v^2 + \{e_b - e_b[(\sqrt{3}/3)\sin\alpha + (1-\cos\alpha)]\}^2$$
$$(\text{K–O})^2_{\text{out}} = v^2 + \{e_b + e_b[(\sqrt{3}/3)\sin\alpha - (1-\cos\alpha)]\}^2 \quad (5)$$

where

$$v = 0{\cdot}5[c\sin\beta - 2d_o\cos\psi - (\tfrac{8}{3})Hd_t] .$$

The subscripts 'in' and 'out' for (K–O) denote the potassium–oxygen interatomic distances for the inner and outer octahedron, respectively. The old formulae used by Donnay *et al.* (1964) can be obtained by substituting 1 for E and H in the above formulae.

The octahedral flattening angle for the inner octahedron of the interlayer cation (potassium), Φ, defined by Takeda & Donnay (1966) in a similar manner as ψ is defined for the octahedral cations (Mg), is given by:

$$\sin^2\Phi = 4/[3(1+r_i^2)] \quad (6)$$

where

$$r_i = (\text{O–O})_t/(\text{O–O})_b ,$$

in which

$$(\text{O–O})_t = 4(\text{K–O})^2_{\text{in}} - (\text{O–O})^2_b$$

and

$$(\text{O–O})_b = 2e_b\cos(30^\circ + \alpha)$$

and where $(\text{O–O})_t$ and $(\text{O–O})_b$ are the appropriate oxygen–oxygen lateral and base interatomic distances about the potassium ion, respectively.

Experimental and structure refinement

Crystal specimens of fluorphlogopite, $KMg(Si_3Al)O_{10}F_2$, used in this study (supplied by Dr M. Ross) were synthesized at the Bureau of Mines and should be the same as those used by McCauley, Newnham & Gibb (1973). A single-crystal fragment of the mica sheet was mounted in the high-temperature furnace described elsewhere (Lynch & Morosin, 1971). The furnace can then be mounted on a Picker four-circle diffractometer. The cell dimensions (Table 1) were obtained by a least-squares fit on more than 15 high 2θ values measured with Cu $K\alpha$ ($\lambda_1 = 1{\cdot}54050$ Å) radiation on the diffractometer at various temperatures between 24 and 800 °C. Two sets of single-crystal Mo $K\alpha$ X-ray intensity data were measured, one for 458 reflections at 24 °C and the other for 434 reflections at 700 °C. Of these, seven and 41 at 24 and 700 °C, respectively, were found to be less than 3σ and were considered unobserved in subsequent calculations. The intensities were reduced to structure factors by applying Lorentz, polarization and absorption factors.

The two data sets were subjected to full-matrix least-squares refinement on a CDC 6600 computer, employing the X-RAY 70 system (Stewart, Kundell & Baldwin, 1970), and on a HITAC 8700/8800 computer, employing the MINEPAC system (Miyamoto, Takeda & Takano, 1974). Initial positional parameters, with isotropic temperature factors, were taken from those of

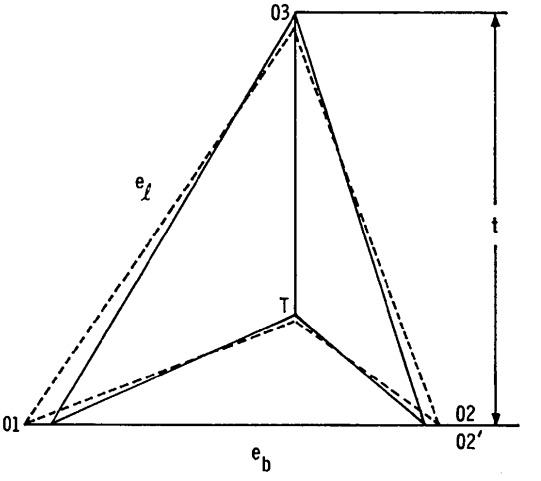

Fig. 2. Relationship of the length of the edges and height for the silica tetrahedra employed in the generalized model. Solid lines indicate tetrahedra in real structures, resulting in a slightly longer height and shorter length for e_b than those of an ideal (regular) tetrahedron in dashed lines.

Table 1. *Cell dimensions, volumes and the assumed* Mg–O *distances* (d_o) *used for predicting the structure at high temperatures*

Standard deviations are in parentheses.

Temperature (°C)	a (Å)	b (Å)	c (Å)	β (°)	V (Å^3)	d (Å)
24	5·3074 (6)	9·195 (2)	10·134 (1)	100·08 (1)	487·01	2·075
142	5·3147 (7)	9·206 (3)	10·154 (1)	100·085 (15)	489·07	2·078
160	5·3148 (7)	9·204 (3)	10·157 (1)	100·09 (1)	489·14	2·0785
202	5·318 (1)	9·207 (4)	10·162 (2)	100·07 (1)	489·90	2·0795
225	5·319 (1)	9·218 (4)	10·172 (2)	100·07 (1)	491·10	2·080
249	5·319 (1)	9·214 (3)	10·173 (2)	100·08 (1)	490·78	2·081
400	5·326 (1)	9·230 (5)	10·203 (2)	100·055 (10)	493·72	2·0845
500	5·330 (1)	9·229 (5)	10·221 (2)	100·055 (10)	495·05	2·087
600	5·335 (1)	9·233 (4)	10·237 (2)	100·025 (10)	496·56	2·0895
710	5·337 (1)	9·240 (4)	10·253 (2)	100·00 (1)	497·98	2·092
802	5·339 (1)	9·246 (5)	10·273 (3)	99·99 (2)	499·42	2·0945
900*	5·345	9·248	10·290	99·96	500·98	2·097

* Extrapolated.

synthetic lithium fluorphlogopite (Takeda & Donnay, 1966). In the final stages of the refinements, a correction for secondary extinction was also applied; however, the residual $R=\sum||F_o|-|F_c||/\sum|F_o|$, did not decrease significantly. The conventional unweighted residuals for the final refinements with anisotropic temperature factors are 0·043 and 0·095 on the properly observed reflections for the 24 and 700 °C data, respectively. The structural parameters are given in Table 2 and the bond lengths are listed in Table 3 with their associated standard deviations.* Our structure refinement on the

* A list of structure factors has been deposited with the British Library Lending Division as Supplementary Publication No. SUP 31048 (9 pp.). Copies may be obtained through The Executive Secretary, International Union of Crystallography, 13 White Friars, Chester CH1 1NZ, England.

Table 2. *Atomic positional and thermal parameters at* 24 °C (*first line*) *and* 700 °C (*second line*)

	x	*y*	*z*	B (Å²)
K	0	0·5	0	2·31 (3)
				6·6 (2)
Mg(1)	0	0	0·5	0·76 (4)
				2·0 (1)
Mg(2)	0	0·3309 (1)	0·5	0·70 (3)
		0·3315 (6)		2·4 (1)
F	0·1332 (4)	0·5	0·4026 (2)	0·86 (4)
	0·1378 (17)		0·3968 (10)	2·7 (2)
(Si_3Al)	0·0755 (1)	0·1666 (1)	0·2253 (1)	0·66 (3)
	0·0732 (5)	0·1664 (3)	0·2267 (3)	2·15 (8)
O(1)	0·0234 (7)	0	0·1663 (3)	1·40 (6)
	0·0401 (22)		0·1689 (13)	3·3 (3)
O(2)	0·3228 (4)	0·2335 (3)	0·1671 (2)	1·30 (5)
	0·3082 (17)	0·2422 (11)	0·1706 (8)	3·5 (2)
O(3)	0·1299 (4)	0·1663 (2)	0·3912 (2)	0·76 (4)
	0·1283 (11)	0·1654 (8)	0·3897 (8)	2·1 (1)

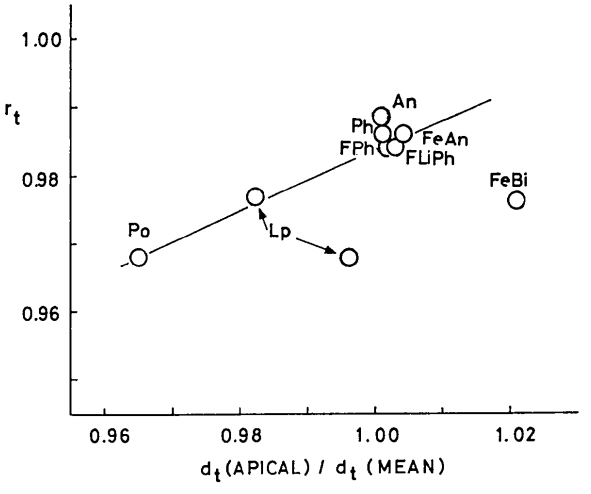

Fig. 3. Typical values of r_t as a function of the ratio d_t (apical)/d_t (mean). The value r_t is the ratio e_b/e_l (see Fig. 2 and text). The following micas are shown: Po = polylithionite (Takeda & Burnham, 1969); Lp = lepidolite $2M_2$ (Takeda, Hega & Sadanaga, 1971); FLiPh = lithium fluorphlogopite (Takeda & Donnay, 1966); Ph = phlogopite (Joswig, 1972); FeAn = ferriannite (Donnay *et al.*, 1964); FPh = fluorphlogopite (this study); An = annite (Hazen & Burnham, 1973); and FeBi = iron biotite (Tepikin, Drits & Alexandrova, 1969).

Table 3. *Selected observed bond distances* (Å) *and angles* (°) *of fluorphlogopite at* 24 *and* 700 °C

		24 °C	700 °C
Tetrahedral parameters			
Si–O(1)		1·650 (1)	1·646 (5)
Si–O(2)		1·650 (2)	1·626 (9)
Si–O(2′)		1·647 (2)	1·662 (8)
Si–O(3)		1·656 (2)	1·647 (9)
Mean		1·651	1·645
O(1)–O(2)		2·671 (3)	2·655 (11)
O(1)–O(2′)		2·672 (3)	2·686 (11)
O(2)–O(2)		2·671 (1)	2·672 (1)
Mean		2·671	2·671
O(3)–O(1)		2·722 (3)	2·704 (13)
O(3)–O(2)		2·722 (3)	2·688 (11)
O(3)–O(2′)		2·715 (3)	2·714 (11)
Mean		2·720	2·702
r_t (Å)		0·982	0·989
O(2)–O(1)–O(2)	2×	107·04 (15)	114·9 (6)
O(1)–O(2)–O(2)	4×	107·01 (14)	114·4 (6)
		107·02	114·57
O(2)–O(1)–O(2)	2×	132·97 (16)	125·0 (6)
O(1)–O(2)–O(2)	4×	132·98 (15)	125·6 (7)
		132·98	125·4
α (°)		6·5	2·7
Octahedral parameters		24 °C	700 °C
Mg(1)–O(3)	4×	2·072 (2)	2·086 (7)
Mg(1)–F	2×	2·023 (2)	2·036 (10)
Mean		2·056	2·069
Mg(2)–O(3)	2×	2·060 (2)	2·091 (8)
M(g2)–O(3′)	2×	2·077 (2)	2·106 (6)
Mg(2)–F	2×	2·034 (2)	2·087 (7)
Mean		2·057	2·095
Mg–O, mean		2·070	2·094
Around Mg(1)			
O(3)–O(3) (shared)	2×	2·805 (4)	2·840 (15)
O(3)–F	2×	2·713 (3)	2·781 (11)
O(3)–O(3) (unshared)	2×	3·058 (2)	3·056 (14)
O(3)–F	4×	3·067 (3)	3·043 (10)
Around Mg(2)			
O(3)–O(3) (shared)	2×	2·797 (4)	2·868 (15)
O(3)–O(3′)	1×	2·805 (4)	2·840 (15)
F——O(3)	2×	2·713 (3)	2·781 (11)
F——F	1×	2·622 (5)	2·778 (17)
O(3)–O(3) (unshared)	2×	3·068 (2)	3·093 (7)
O(3)–F	2×	3·063 (3)	3·093 (7)
O(3′)–F	2×	3·070 (2)	3·109 (10)
Interlayer parameters		24 °C	700 °C
K–O(1)	2×	2·986 (3)	3·095 (11)
K–O(2)	4×	2·987 (2)	3·121 (9)
Mean (in)		2·987	3·112
K–O(1)	2×	3·276 (3)	3·240 (13)
K–O(2)	4×	3·285 (2)	3·231 (10)
Mean (out)		3·282	3·234
Around K			
O(1)–O(2)	4×	4·151 (4)	4·282 (14)
O(2)–O(2′)	2×	4·152 (4)	4·349 (16)
Mean (lateral)		4·151	4·304
O(1)–O(4)	4×	4·295 (4)	4·505 (15)
O(2)–O(2′)	2×	4·295 (5)	4·476 (20)
Mean (basal)		4·295	4·495
l/*b*		0·966	0·958
O(1)–O(1)	2×	3·336 (6)	3·416 (27)
O(2)–O(2)	4×	3·352 (4)	3·448 (15)
Mean (shortest interlayer distances)		3·347	3·437

24 °C data was carried out prior to the publication of the study by McCauley, Newnham & Gibb (1973) (these authors used a crystal with a slight stacking disorder); the room-temperature refinement is in good agreement with that study. The positional parameters determined at 700 °C which differ by more than 3σ from the 24 °C values are the x parameters of O(1), O(2) and y of O(1). These shifts of coordinates are those necessary for the ditrigonal oxygen ring to become more nearly hexagonal.

Prediction of high-temperature structural parameters

The geometrical model requires the use of lattice constants at the temperature of interest, the room-temperature bond distances and mean thermal expansivities for similar bond lengths. The observed values for b and $c \sin \beta$ given in Table 1 were the values used together with a value for $d_t = 1{\cdot}649$ Å, obtained by refinement of the room-temperature structure, which was used throughout the temperature interval to 900 °C. This latter assumption of a constant size for the tetrahedron is based upon the results found in the high-temperature pyroxene and amphibole structures (Cameron *et al.*, 1973) in which the cation–oxygen distances were not significantly different from room-temperature values. The d_o values (Table 1) were obtained by applying the mean thermal expansion coefficient (MTEC) of the mean [M(1), M(3)–O] distance determined in tremolite (Sueno, Cameron, Papike & Prewitt, 1973) to our observed room-temperature Mg–O distance. The M(1) and M(3) octahedra in tremolite are probably the most similar to those in micas (Takeda & Morimoto, 1970) that are currently available in refined high-temperature structures. The tetrahedral correction factor, $r_t = 0{\cdot}984$, is obtained from our preliminary room-temperature structure refinement and is in general agreement with values shown in Fig. 3 (see caption).

The predicted structural parameters, consisting of the tetrahedral rotation angle α, the octahedral flattening angles for both the Mg and K octahedra and the inner K–O distances were computed by equations (3), (4), (6) and (5), respectively, on a HITAC 8700/8800 computer. These predicted values are shown in Figs. 6 and 7 and will be discussed and compared with our experimental values in the next section.

Results

The cell dimensions and the resulting volume (Table 1) are plotted as a function of temperature in Fig. 4. The rate of increase of the a and b axis lengths (or edges) decreases at about 400 °C, while the rate of change of the angle β becomes larger at about the same temperature. On the other hand, the c axis length increases constantly, with a linear expansivity value nearly twice as large as that along the other cell dimensions. The larger expansivity along the c axis dominates the volume expansivity such that the kink in the cell volume is not too striking. The values ($\times 10^5\,°C^{-1}$) for

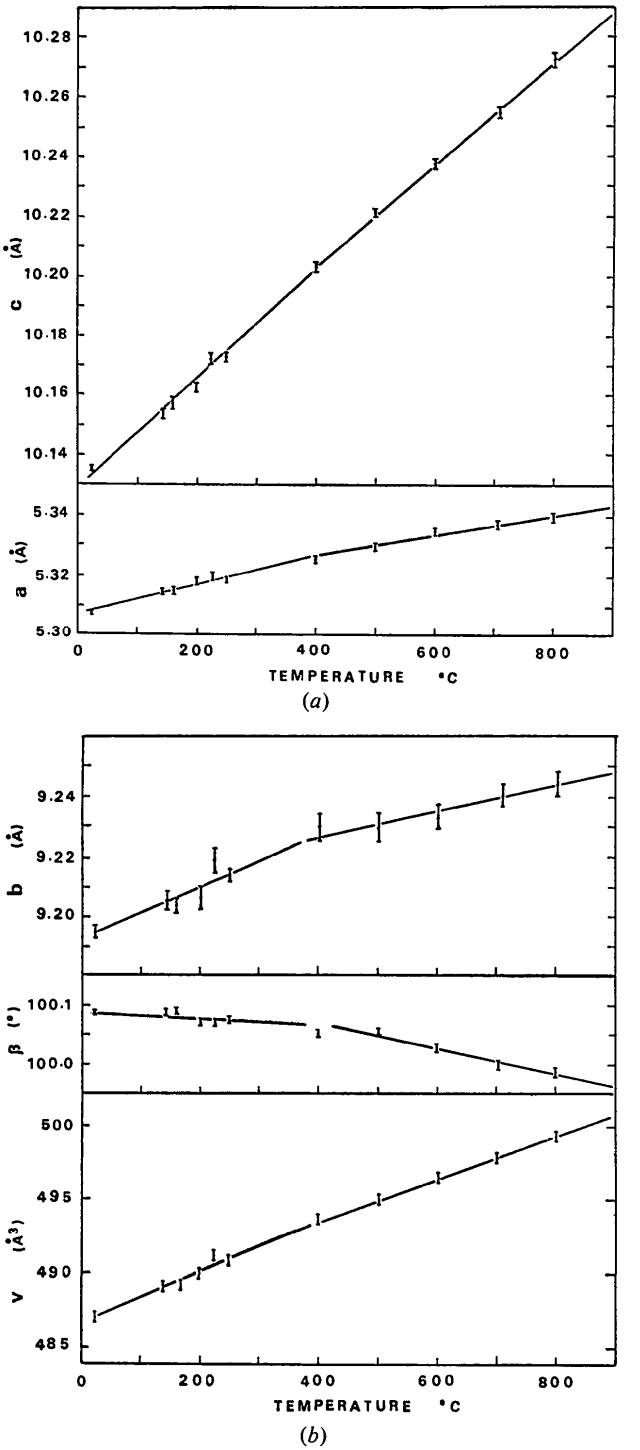

Fig. 4. Cell dimensions as a function of temperature for fluorphlogopite. The indicated error bars on values are the standard deviations determined from the least-squares fit on 2θ values measured. The linear expansivities (slopes of these lines) are given in the text. Note the kink in the slopes near 400 °C.

the linear thermal expansivities $\alpha_x=(1/X_{24})(X_T-X_{24})/(T-24)$°C along **a**, **b**, and **c** are 0·98, 0·93 and 1·73, respectively, over the temperature interval 24–350°C and 0·62, 0·48 and 1·70, respectively, between 400–800°C. The corresponding volume expansivities are 3·91 and 3·06 for the low- and high-temperature intervals, respectively.

The predicted values for the angle α decrease almost linearly from 6·4° at 24°C to 1·8° at 900°C (Fig. 5); extrapolation of the values suggests that α may become 0° above 1200°C. The observed angle of 2·7° at 700°C agrees with the calculated value of 3°. As noted above, the differences in the observed positional parameters between 24 and 700°C are directly related to the ditrigonal oxygen ring tending toward hexagonal.

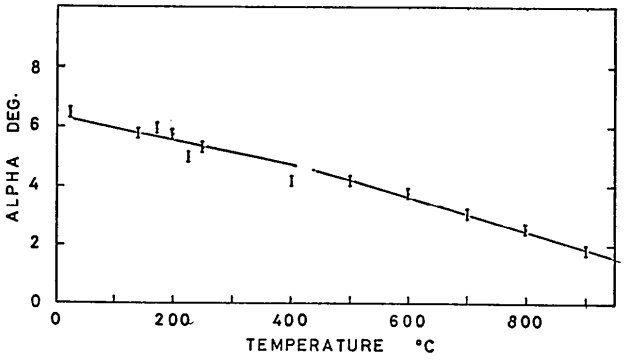

Fig. 5. Calculated values for the angle α as a function of temperature for fluorphlogopite. Straight line represents visual fit to calculated points without step discontinuities.

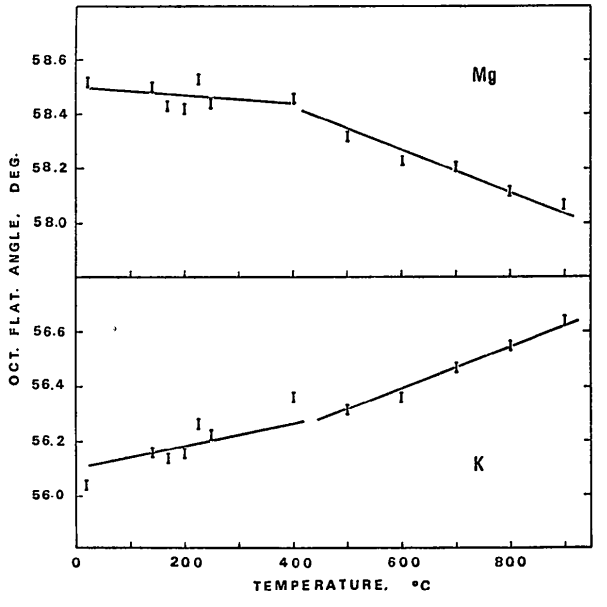

Fig. 6. Calculated values for the flattening angle of the Mg and K octahedra for fluorphlogopite. Straight line represents a visual fit to the calculated points. The K^+ ion has six closer (inner) distances and six more distant neighbors; the inner set are considered to form the octahedron.

The octahedral flattening angle for the Mg octahedron is nearly constant for values to 400°C, but decreases *sharply* above this temperature (Fig. 6). The observed ψ angle 58·5° at 24°C and 58·0° at 700°C confirms this trend. The calculated angles for the inner oxygen octahedron about the potassium ion are also shown in Fig. 6 and found to increase in both temperature intervals; the rate of increase in the higher temperature interval is slightly larger. The observed value is 56·2° at 24°C and 56·5° at 700°C, in agreement with predicted values.

The predicted values for the K–O interatomic distances are shown on Fig. 7. A value for the MTEC of the K–O distance derived from such predicted values is in good agreement with that from the refined K–O bond lengths of 2·987 Å at 24° and 3·112 Å at 700°C [*i.e.* $6\times10^{-5}(°C)^{-1}$] (Table 5). The assumed MTEC of the Mg–O distance [$1{\cdot}21\times10^{-5}(°C)^{-1}$] was derived from the observed values for the M(1) and M(3) octahedra in tremolite (Sueno *et al.*, 1973, Table 4). This value agrees with the observed value computed from our refined crystal structures at 24 and 700°C. The T–O separations of 1·651 Å at 24°C and of 1·645 Å at 700°C are also indicated on Fig. 7; however, as indicated above, the model employed a constant value over the temperature range of interest. The slight shortening of the high-temperature value may partly be due to the increased π-bond order required with larger T–O–T angles with increasing temperature, as had been proposed for the orthopyroxene structure (Takeda, 1974).

Discussion

The relationship between the mode of the deformation of the mica structure by isomorphous substitution, as

Table 4. M(1)–O *and* M(3)–O *distances* (Å) *of tremolite* (*Sueno et al.*, 1973) *used to derive the values for* Mg–O *distances of each octahedron at* 24, 400 *and* 700°C

Distance	24°C	400°C	800°C
M(1)–O(1) mean	2·075	2·084	2·094
M(3)–O(1) mean	2·066	2·076	2·082
[M(1), M(3)]–O(1) mean	2·071	2·080	2·088

Table 5. *Bond distances* (Å) *used to compute the mean thermal expansion coefficient* (*MTEC*) *of fluorphlogopite and* M(1,3)–O *of tremolite*

Distances	24°C	700°C	MTEC [$\times10^5(°C)^{-1}$]
Tremolite			
M(1,3)–O	2·071	2·088	1·21
Fluorphlogopite			
Mg–O	2·070	2·094	1·72
Mg–O, F	2·057	2·086	2·08
K–O (in)	2·987	3·112	6·19
K–O (in, pred.)	2·990	3·099	5·39

well as the polymorphism or polytypism exhibited by micas has been a subject of extensive studies in the last decade. However, what may affect the formation of mica polytypes is the mode of deformation at high temperatures where the crystal growth is actually taking place. Our results indicate that the oxygen ring formed by the tetrahedra approaches that of a hexagon at high temperature. Since it is anticipated that for most of the trioctahedral micas this ring will be close to hexagonal at high temperature, lack of polytypism based on 60–180° interlayer rotations, in micas other than lithium-bearing members, needs to be explained in terms of other factors besides the non-hexagonality of the ring. For example, such factors could possibly be those previously suggested, such as the interaction of potassium and hydroxyl or fluorine ions or the neutrality of the surface oxygen rings (Takeda & Burnham, 1969; Takeda, Haga & Sadenaga, 1971). At any rate, good agreement between the observed and predicted parameters suggests that the improved geometrical mica model (Takeda, 1971) will be useful in obtaining structural parameters at high temperatures without performing high-temperature refinements for each mica in question.

Furthermore, the changes in the linear thermal expansivities of fluorphlogopite suggest that there may be a high-temperature form of mica obtained without symmetry change. The mode for structural changes at temperatures above 400°C is quite different from that below this temperature. In particular, the Mg octahedron expands without changing its shape at temperatures below 400°C. Then, above this temperature the Mg octahedra begin to elongate more rapidly perpendicular to the layer.

From the studies of the structural changes resulting from the substitution of larger ions for smaller ones, it was anticipated that this Mg octahedron would expand without deformation until the oxygen ring attains the ideal hexagonal shape. However, our results show that the α values change almost linearly throughout the temperature interval 24–900°C (1200°C is needed for the ring to become hexagonal) whereas the octahedron begins to elongate above 400°C. Evidently the internal forces acting on the octahedron are sufficiently large to cause deformation before the ring reaches the ideal hexagonal form. From this observation, it can be stated that the octahedral coordination of the inner oxygen atoms around the potassium ion is preferred rather than increasing to 12-fold or larger coordination even at the expense of elongation of the octahedron.

We noted above that the linear thermal expansivity along the c axis is approximately twice as large as those along the other cell dimensions. The major contribution of this expansion can be ascribed to the expansion of the K octahedra. As noted above, the MTEC of the K–O distance is four times greater than that of the Mg–O distance.

This large MTEC of the K–O distance is related to several factors. The force constants for interatomic distances show an inverse relationship with MTEC values (Alekhina & Akhmanova, 1971). For example,

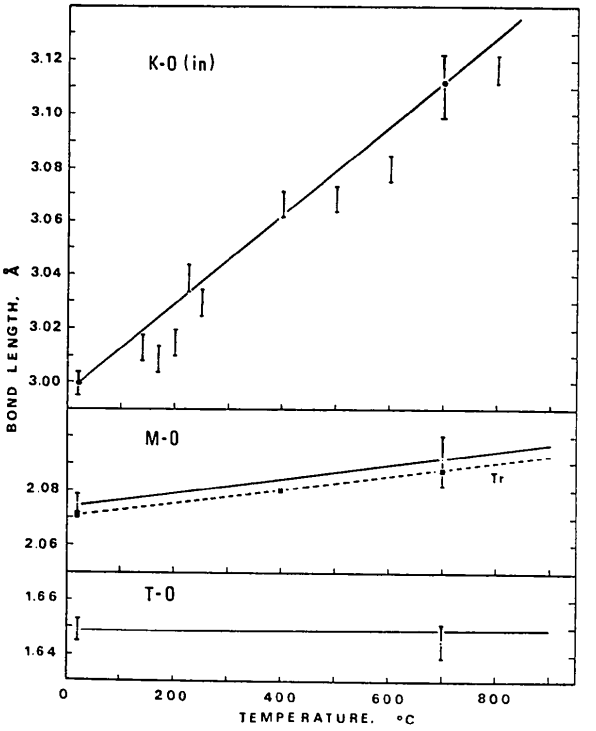

Fig. 7. Calculated interatomic distances (Å). The values for the K–O distance (top) are shown with a straight line drawn through the 24 and 700°C experimentally determined values. The straight line shown for the M–O distance (middle) represents the values used in the model with MTEC from tremolite; actual experimental values are shown as well as the values determined in tremolite (Tr) through which a dashed line is drawn. The T–O distance (bottom) was assumed constant in the model and this is indicated by the straight line; the two experimental points determined at 24 and 700°C are shown (error determined from the least-squares analysis of refined intensity data).

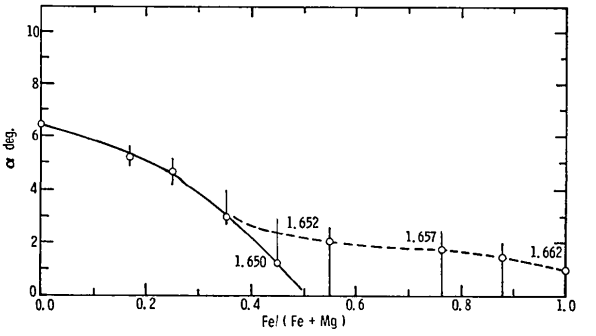

Fig. 8. Values of α in the biotite solid-solution series as a function of Fe substitution. Vertical bars define possible limits in predicted values; d_t values are indicated to span estimated data from the biotite series, *i.e.* 1·650 Å for the solid curve while other values over the dotted curve are necessitated by the increased Fe^{3+} concentration as one tends towards the Fe-rich series.

the force constant obtained in phlogopite by far-infrared spectroscopy for the K–O distance is 0·05 mdyn $Å^{-1}$ (Ishii, Shimanouchi & Nakahira, 1967), a much smaller value than either for the Si–O (3·508) or Mg–O (0·320) bond distances. Similarly, the larger temperature factors of interlayer cations (*ca.* $B=2$ Å^2) appear to be related to the larger MTEC values. Because the interlayer distance becomes much larger with increasing temperature, it appears that this weak bond will probably be the first to be broken when the crystal begins to melt.

The method for predicting certain structural parameters at high temperature, using MTEC of the octahedral cation-to-anion distances of the related compounds, appears to be useful in deducing the relationship between the structural changes at high temperature and the polytype formation. Similar approaches can probably also be applied to other groups of minerals once a probable model structure has been established.

Comments on chemical expansion

Let us now consider the resulting expansion in micas which is attained when larger ions are substituted in the Mg octahedron, what may be called the 'chemical expansion' of polyhedra. As mentioned above, such results suggested a uniform expansion of the Mg octahedron with temperature contrary to our findings. The initial structural modeling to encompass chemical substitution rested on the premise that there existed a misfit between the octahedral and tetrahedral layers in the sheet silicates primarily because it was generally understood that the octahedron is a rigid body. Donnay *et al.* (1964) introduced the parameter ψ in order to determine the amount of flattening of the octahedron caused by cation–cation repulsion in such misfit interfaces. However, our results suggest that in some cases the octahedron must elongate along the $\bar{3}$ axis prior to the ring attaining a hexagonal form. In such structures, the octahedron before elongation is too large to fit the observed *b* axis length. This suggests that micas with considerable amounts of larger cations, such as manganese, substituted isomorphously in the octahedral layer would show such octahedral elongation.

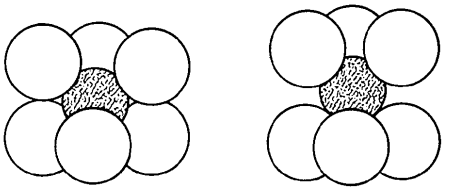

Fig. 9. Sketch illustrating the difference in the K octahedron as a function of Fe substitution in the biotite series. That for annite (left side) is much more flattened than the nearly regular one for phlogopite (right).

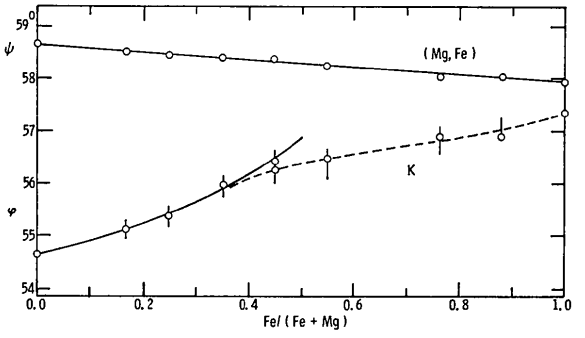

Fig. 10. Values of ψ for (Mg, Fe) octahedra and of Φ for K octahedra in the biotite series as a function of Fe substitution. Vertical bars for Φ values are estimated error limits in predicted values. The solid line is that corresponding to $d_t=1{\cdot}650$ while the dotted line spans d_t values as given in Fig. 8.

The suggested basis for differential polyhedral expansion found in pyroxenes and amphiboles at high temperature (Smyth & Burnham, 1972; Cameron *et al.*, 1973) appears to have a parallel trend in mica crystal chemistry (Donnay *et al.*, 1964). However, in micas the expansion is mainly due to replacement of the smaller cations by larger cations.

In the biotite series, the replacement of Mg^{2+} by Fe^{2+} (a slightly larger cation) in the octahedra probably results in a differential polyhedral expansion between the octahedral layer and the tetrahedral layer. As a consequence of this chemical expansion, the oxygen rings tend towards the ideal hexagonal form as one proceeds towards the Fe-rich members. The calculated α angles reveal this trend, as is shown in Fig. 8 which was constructed by employing *b* and $c \sin\beta$ values from Wones (1963), the r_t values of phlogopite (Joswig, 1972) and annite (Hazen & Burnham, 1973), and the known atomic distances. The dotted line in Fig. 8 shows the effect of increased Fe^{3+} substitution in the tetrahedral site as the composition tends towards annite; the average T–O distance increases approximately as indicated. Because of this chemical expansion of the Mg-type octahedron, the K atom can be situated in a larger open hole, and in order to attain the proper K–O distance the K–O octahedron must flatten more with increasing Fe concentration (Fig. 9). The corresponding values for ψ and Φ for the (Mg, Fe) and the K octahedra, respectively, are given in Fig. 10. Note that the ψ values tend to decrease slightly with increasing Fe concentration. Thus, the substitution of Fe for Mg results in an expansion of the Mg–O type octahedron, with the K octahedron tending to flatten without pronounced expansion. This flattening accounts for the almost constant *c* axis dimension of the biotite solid-solution series, in spite of the expected chemical expansion by the larger cations. This results in a major difference in that chemical substitution results in a negligible expansion compared with the rather extensive expansion along **c** resulting from heating the crystals.

Conclusions

We conclude the following about fluorphlogopite: (1) the surface oxygen rings of the tetrahedral layer approach a hexagonal form with increasing temperature; (2) the expansion of the K–O distance is much larger than that of the Mg–O distance; and (3) with increasing temperature the Mg octahedron expands freely; however, it begins to elongate perpendicular to the layer long before the ring attains a hexagonal form. The substitution of Fe for Mg in biotites causes the K octahedron to flatten, yielding an almost constant *c* axis length throughout the solid solution series. Thus, this negligible expansion resulting from chemical substitution is in marked contrast to the large *c* axis expansivity caused by heating.

Part of this study was carried out at the NASA Manned Spacecraft Center, where one of the authors (H.T.) was a senior resident research associate of the NRC. The work was supported in part by the U.S. Atomic Energy Commission. Thanks are also due to Drs M. Ross and J. W. McCauley for supplying the specimen of synthetic fluorphlogopite, R. A. Trudo for experimental assistance, Professors R. Sadanaga and Y. Takéuchi for interest and support of this work, and Professor J. J. Papike and Dr S. Sueno for providing us with their tremolite data prior to its publication.

References

ALEKHINA, L. G. & AKHAMANOVA, M. V. (1971). *Geochem. Int.* **8**, 504–510.

CAMERON, M., SUENO, S., PREWITT, C. T. & PAPIKE, J. J. (1973). *Amer. Min.* **58**, 594–618.

DONNAY, G., DONNAY, J. D. H. & TAKEDA, H. (1964). *Acta Cryst.* **17**, 1374–1381.

DRITS, V. A. (1969). *Proc. Int. Clay Conf. Tokyo*, **1**, 51–59. Israel Univ. Press.

FRANZINI, M. & SCHIAFFINO, L. (1963). *Z. Kristallogr.* **119**, 297–309.

HAZEN, R. M. & BURNHAM, C. W. (1973). *Amer. Min.* **58**, 889–900.

HAZEN, R. M. & WONES, D. R. (1972). *Amer. Min.* **57**, 103–125.

ISHII, M., SHIMANOUCHI, T. & NAKAHIRA, M. (1967). *Inorg. Chem. Acta*, **1**, 387–392.

JOSWIG, W. (1972). *Neues Jb. Miner. Mh.* pp. 1–11.

LYNCH, R. W. & MOROSIN, B. (1971). *J. Appl. Cryst.* **4**, 352–356.

MCCAULEY, J. W. & NEWNHAM, R. E. (1971). *Amer. Min.* **56**, 1626–1638.

MCCAULEY, J. W., NEWNHAM, R. E. & GIBB, G. U. (1973). *Amer. Min.* **58**, 249–254.

MIYAMOTO, M., TAKEDA, H. & TAKANO, Y. (1974). *Sci. Pap. College Gener. Ed. Univ. Tokyo*, **24**, 115–126.

MOROSIN, B. (1972). *Acta Cryst.* B**28**, 1899–1903.

RADOSLOVICH, E. W. (1960). *Acta Cryst.* **13**, 919–932.

RADOSLOVICH, E. W. & NORRISH, K. (1962). *Amer. Min.* **47**, 599–616.

SMYTH, J. R. & BURNHAM, C. W. (1972). *Earth Planet. Sci. Lett.* **14**, 183–189.

STEWART, J. M., KUNDELL, F. A. & BALDWIN, J. C. (1970). X-RAY 70, a System of Crystallographic Computer Programs. Univ. of Maryland, College Park, Maryland.

SUENO, S., CAMERON, M., PAPIKE, J. J. & PREWITT, C. T. (1973). *Amer. Min.* **58**, 649–664.

TAKEDA, H. (1971). *Geol. Soc. Amer. Abs. Annual Meeting*, **3**, pp. 727–728.

TAKEDA, H. (1974). *Symp. Proc. Exp. Petrol.* pp. 193–204. Sendai, Japan: Soc. Pet. Miner. Econ. Geol.

TAKEDA, H. & BURNHAM, C. W. (1969). *Miner. J.* **6**, 102–109.

TAKEDA, H. & DONNAY, J. D. H. (1966). *Acta Cryst.* **20**, 638–646.

TAKEDA, H., HAGA, N. & SADANAGA, R. (1971). *Miner. J.* **6**, 203–215.

TAKEDA, H. & MORIMOTO, N. (1970). *J. Cryst. Soc. Japan*, **12**, 231–248.

TAKÉUCHI, Y. (1964). *Proc. Nat. Conf. Clays Clay Miner.* **13**, 1–25.

TEPIKIN, E. V., DRITS, V. A. & ALEXANDROVA, V. A. (1969). *Proc. Int. Clay Conf. Tokyo*, **1**, 43–49. Israel Univ. Press.

WONES, D. R. (1963). *Amer. Min.* **48**, 1300–1321.